Earth's Future

RESEARCH ARTICLE
10.1029/2022EF002649

Predominant Type of Dust Storms That Influences Air Quality Over Northern China and Future Projections

Jiandong Li[1], Xin Hao[1,2,3], Hong Liao[1], Xu Yue[1], Hua Li[2,3], Xin Long[4], and Nan Li[1]

[1]Jiangsu Key Laboratory of Atmospheric Environment Monitoring and Pollution Control, Jiangsu Collaborative Innovation Center of Atmospheric Environment and Equipment Technology, School of Environmental Science and Engineering, Nanjing University of Information Science and Technology, Nanjing, China, [2]Center for Climate System Prediction Research/Collaborative Innovation Center on Forecast and Evaluation of Meteorological Disasters/Key Laboratory of Meteorological Disaster, Ministry of Education, Nanjing University of Information Science and Technology, Nanjing, China, [3]Nansen-Zhu International Research Centre, Institute of Atmospheric Physics, Chinese Academy of Sciences, Beijing, China, [4]Chongqing Institute of Green and Intelligent Technology, Chinese Academy of Sciences, Chongqing, China

Key Points:

- Spring dust storms in northern China were clustered into two types driven by Mongolian cyclone and cold front
- Mongolian cyclone caused dust storm is the predominant type influencing air quality in northern China
- Mongolian cyclone caused dust storms will decline under global warming, but fluctuate if global warming is mitigated

Supporting Information:

Supporting Information may be found in the online version of this article.

Correspondence to:

H. Liao,
hongliao@nuist.edu.cn

Citation:

Li, J., Hao, X., Liao, H., Yue, X., Li, H., Long, X., & Li, N. (2022). Predominant type of dust storms that influences air quality over northern China and future projections. *Earth's Future*, *10*, e2022EF002649. https://doi.org/10.1029/2022EF002649

Received 4 JAN 2022
Accepted 27 MAY 2022

Abstract Dust storms (DSs) originating in East Asia impact ecosystems, climate, and public health in China. Although DS frequencies have declined since the 1950s, extreme DSs in spring 2021 had major effects on air quality over northern China. Based on daily DS records in spring during 1979–2021 and *K*-means clustering, we define two DS types (T1 and T2) in northern China, accounting for 18.7% and 81.3% of DSs, respectively. T1 DSs, originating mainly in the Gobi Desert, predominantly influence air quality in northern China, while T2 DSs mainly influence northwestern China near the Taklimakan Desert. T1 and T2 DSs are driven by major synoptic systems including the Mongolian cyclone and cold fronts, respectively. Based on predictions of the Climate Models Intercomparison Project Phase Six, we demonstrate that the spring DS frequency would decrease during 2020–2100 under the shared socioeconomic pathway (SSP) 585 scenario but would fluctuate with decadal variability under the SSP126 scenario. Our results indicate that spring DSs can be triggered by a range of mechanisms, with distinct impacts on air quality.

Plain Language Summary Dust storms (DSs) in China have been declining since the 1950s. The severe DSs of spring 2021 aroused public concern regarding future changes in DSs. Based on DS records for 1979–2021, spring DSs were clustered into two types driven by different weather systems, namely Mongolian cyclones and cold fronts. The former type is less common but plays a dominant role in the deterioration of air quality over northern China. With the help of state-of-the-art climate models, we estimated that Mongolian-cyclone-driven DSs will decrease in frequency during 2020–2100 with global warming, but would fluctuate decadally if global warming is mitigated.

1. Introduction

Dust storms (DSs) have adverse impacts on climate (Liao & Seinfeld, 1998; Sokolik & Toon, 1996), ecosystems (Griffin et al., 2001), and human health (Fussell & Kelly, 2021; Ichinose et al., 2008). East Asia is a major source of dust aerosol, contributing ~25% of total annual global dust emissions (Yao et al., 2021). The major dust sources in East Asia are the Taklimakan Desert (TD) in northwestern China and the Gobi Desert (GD) in southern Mongolia and parts of northern and northeastern China (Sun et al., 2001).

DSs occur through the combined effects of surface conditions and meteorological factors. Surface conditions such as vegetation cover (Fan et al., 2014; Ji & Fan, 2019; Zou & Zhai, 2004), soil, and topography (Chen et al., 2017; Engelstaedter et al., 2003) play important roles in dust emission via sand initiation processes. Meteorological factors affect both these processes and the transport of DSs. Wind speed is the dominant factor controlling the frequency of DSs (Lee & Sohn, 2009; Xu et al., 2020). The observed decreasing trend in DS frequency over northern China since the 1970s has been attributed to decreasing surface wind speed (Ding et al., 2005; Guan et al., 2017; Zhao et al., 2004). Other factors, such as temperature (Yin et al., 2021), precipitation (Liu et al., 2004), soil moisture (Yao et al., 2021), and evaporation (Shi et al., 2020), indirectly affect dust emissions by changing the subsurface and dust source conditions. For example, low precipitation and strong evaporation in Mongolia produced dry soil and exiguous vegetation during the spring of 2021, leading to severe DSs in northern China (Yin et al., 2021). DSs occur under various synoptic-scale systems. Earlier studies have found that Mongolian cyclones, cold fronts, and cold highs (Huang et al., 2013; Meng et al., 2019; Yin et al., 2021) are the major

weather systems driving outbreaks of DSs over northern China. It is critical to identify which synoptic system is responsible for dust storms in different subregions.

Observational evidences indicate a remarkable decrease in the frequency of spring DSs in northern China since the 1950s (Guo et al., 2018; Qian et al., 2002; Zhu et al., 2008), but the outbreak of a super DS in northern China during spring 2021 raised concerns as to whether East Asia has entered a period of high-frequency DSs. It is therefore important to project future changes in DS occurrence, although climate change has added complexity to the issue, with simultaneous changes in meteorological factors and dust source conditions under global warming scenarios. Current future projections focus mainly on dust emissions (Wu et al., 2018; Zong et al., 2021), but state-of-the-art climate models participating in CMIP5 and CMIP6 (Climate Models Intercomparison Project phase five/six) are still unable to simulate dust aerosol loadings well for northern China (Pu & Ginoux, 2018; Zhao et al., 2022). For example, Wu et al. (2018) found that the observed trend in dust event frequency from 1961 to 2005 over East Asia could not be reproduced in CMIP5 models. Other studies have focused on future changes in dust source conditions. Huang et al. (2016) projected an expansion of dryland coverage over northern China under a future global warming scenario, indicating worse dust source conditions and more dust storms. However, current prediction research on dust events is relatively lacking. Global climate models rely on many meteorological variables, can be adopted to link DS occurrence to associated synoptic systems for a single process that can be projected under climate change.

Here, using daily DS records for northern China and K-means method, we aim to (a) cluster different DS types and investigate their driving synoptic systems; (b) identify the predominant DS type influencing northern China; and (c) project its future changes based on climate models participating in CMIP6 under climate-change scenarios.

2. Data and Methods

2.1. Meteorology Data, PM_{10} Observations, Normalized Difference Vegetation Index, and Aerosol Optical Depth

In situ observations of surface meteorological variables were obtained from the US National Climatic Data Center (NCDC; https://www.ncei.noaa.gov/data/global-hourly/access/; last accessed 22 April 2022), with wind speed at 10 m, air temperature at 2 m, and horizontal visibility being available for 174 sites (Figure S1 in Supporting Information S1) over northern China.

Daily meteorological variables, including 500 and 850 hPa geopotential heights, zonal and meridional wind speeds at 500, 850 hPa, and 10 m, and mean sea-level pressure, were obtained from the fifth generation of European Center for Medium-Range Weather Forecasts atmospheric reanalyses of the global climate (ERA5) (Hersbach et al., 2020) with a spatial resolution of $1° \times 1°$. Hourly PM_{10} (particulate matter of <10 μm size) concentrations were obtained from the Chinese Ministry of Ecology and Environment (http://106.37.208.233:20035/), with data from continuous measurements at 1500+ sites in 368 major cities in China being available. The quality control and daily average PM_{10} were processed based on the following steps: (1) negative or missing values are excluded from the data; (2) an observation site with less than 80% valid data since the beginning of continuous observations is eliminated; (3) the daily mean PM_{10} concentration of the city is calculated only when there were more than 16 hr of valid data during that day (J. Li, Hao, et al., 2021; J. Li et al., 2019).

To investigate the relationship between DS and dust source regions, gridded monthly Normalized Difference Vegetation Index (NDVI) datasets with a spatial resolution of $1° \times 1°$ were obtained from https://lpdaac.usgs.gov/products/mod13c2v006/.

Daily mean aerosol optical depth (AOD) data with a spatial resolution of $1° \times 1°$ from Level 3 Moderate Resolution Imaging Spectroradiometer Atmosphere Daily Global products (https://ladsweb.modaps.eosdis.nasa.gov/search/) were used in studying the temporal evolution of DSs.

2.2. Dust Storm Definition

The China Meteorological Administration defines a DS event as occurring when visibility is <1 km on an hourly basis. Here, visibility data from 1979 to 2012 were multiplied by 0.766 to correct for the change from manual observation to automatic monitoring since 2013 (H. Li, Yang, et al., 2021; Pei et al., 2018). Additional criteria

were also set with relative humidity <80%, wind speed >3 m s^{-1}, and precipitation = 0 to exclude other meteorological phenomena (e.g., fog, haze, rain) that reduce visibility.

2.3. K-Means Algorithm

To identify the predominant DS type that influences air quality over northern China, the K-means algorithm was used to cluster DS events that occurred during the spring season of March–April–May (MAM) during 1979–2021. This method has been widely applied in studies of extreme events, including heat waves (Agel et al., 2021), extreme precipitation (He et al., 2021), and air pollution (Chang & Zhan, 2017).

For each site, daily sample values were set to 1 when a DS occurred that day, and 0 for non-DS days. The 174 sites were permuted to a 0–1 two-dimensional array (site vs. time) for clustering. Synoptically driven DSs in northern China influence large territories, so daily samples for at least three sites at which a DS occurred were considered for clustering, with 632 daily samples being assigned to specific number clusters by the K-means algorithm. To optimize the classification, a set of classification configurations with numbers of 2–7 was considered, with the two-type configuration being identified as being optimal by Monte Carlo simulation; more meaningful types could not be identified through more classification (Figures S2–S6 in Supporting Information S1). For details of the K-means clustering and Monte Carlo tests, see the Supporting Information S1.

2.4. Mongolian Cyclone Index

In the following analysis, we found that the Type 1 DSs were driven by the Mongolian cyclone. Hence, we applied three meteorological proxies (geopotential height at 850 hPa, Z850; zonal wind at 10 m, U10; and meridional wind at 10 m, V10) to construct a Mongolian Cyclone Index (MCI) to investigate future changes in the MCI under climate change. The Z850 proxy represents the intensity and position of Mongolian cyclones (Qian et al., 2002; Zhu et al., 2008), while U10 and V10 indicate the corresponding near-surface winds identified as the most important factors in modulating the outbreak of Asian dust (Lee & Sohn, 2009). Regional averages were used to create daily time series for meteorological proxies Z850, U10, and V10, which were determined by the most significant anomalies in dust storm composites. Following Cai et al. (2017), we normalized each time series by its respective standard deviation and summed the three normalized time series to construct a single MCI. Due to intra-seasonal variations in spring circulation over East Asia, the MCI was established separately for each month of March, April, and May. In the future projection section, we removed the thermal dilation of Z850 caused by tropospheric warming by subtracting zonal annual means from daily-scale Z850 fields (Zhang et al., 2021) to focus on circulation changes under climate change. To enable a direct comparison, daily Z850, U10, and V10 values were obtained using daily anomalies referenced to the historical 30-year (1981–2010) daily mean, normalized by the historical standard deviation.

2.5. CMIP6 Climate Data

18 CMIP6 model runs (Table S1 in Supporting Information S1) were undertaken where daily outputs of Z850, U10, and V10 were available. We considered two experiments based on SSP126 and SSP585 (Shared Socioeconomic Pathway 1–2.6 and 5–8.5). The SSP126 scenario, with an additional radiative forcing of 2.6 W m^{-2} in 2100, assumes climate mitigation measures being taken to simulate development compatible with limiting the temperature increase to 2°C (Riahi et al., 2017). The SSP585 scenario corresponds to the RCP85 scenario in CMIP5, with an anthropogenic radiative forcing of 8.5 W m^{-2} by 2100, with a 5°C temperature increase (Riahi et al., 2017).

3. Results and Discussion

3.1. DS Types Over Northern China and Associated Weather Conditions

The spatial distribution of composited DS frequencies for 1979–2021 is shown in Figure 1a for T1 and T2 DSs, which account for 18.7% and 81.3% of the 632 spring dust storms (Figure 2a), respectively. Significantly clustered sites of a specific type indicate their co-variability in DS outbreaks (Figure 1a), perhaps involving the same weather system. For T1 DSs, high frequencies occurred over northern China, from the western Inner Mongolia

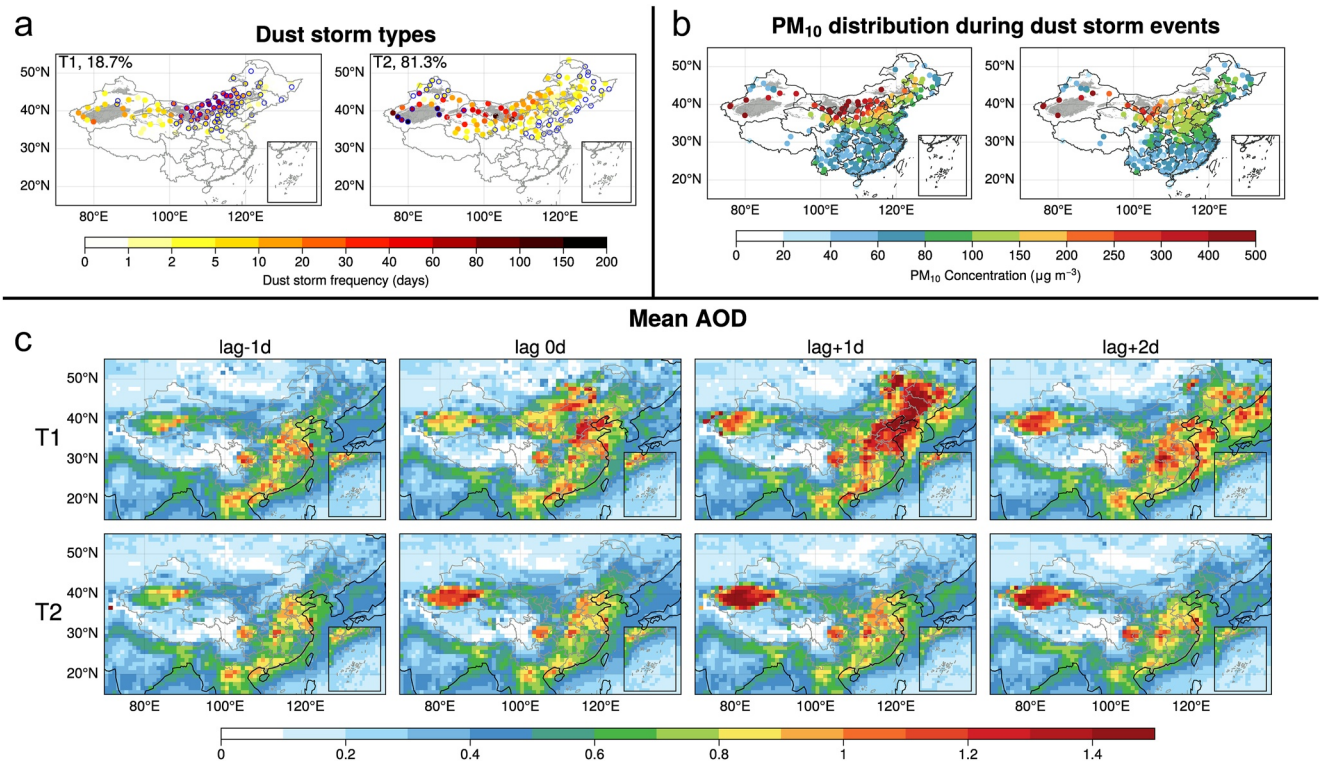

Figure 1. Composites of (a) frequency (days) and (b) mean PM_{10} concentrations (μg m^{-3}) during spring dust storms (DSs) over China during 1979–2021, based on K-means clustering ($k = 2$). (c) Evolution of aerosol optical depth (AOD) for the periods from 1 day before a DS event until 2 days after. Dots with blue circles in (a) indicate sites exceeding the 95% significance level (Monte Carlo test).

Autonomous Region to eastern Hebei Province. These DS "hotspots" were located around the GD (Figure S1 in Supporting Information S1). For T2 DSs, high frequencies occurred over northwestern China, with dust particles being sourced mainly from the TD (Figure S1 in Supporting Information S1), the largest desert in China.

A DS can reduce surface air quality by increasing the concentrations of PM_{10} (Figure 1b). For T1 DSs, the mean PM_{10} concentrations in most regions of northern China were in the range of 200–500 μg m^{-3}, while T2 DSs had a major impact on the air quality over only northwestern provinces. The evolution of AOD during T1 and T2 DSs is illustrated in Figure 1c from 1 day before the DS event (lag−1 day) until 2 days afterward (lag + 2 days). AOD for both T1 and T2 DSs peaked 1 day after the outbreak, before dissipating over 2 days. For T1 DSs, high AOD occurred from northeastern to central China, and for T2 DSs it occurred locally around dust source regions.

Monthly occurrences of T1 and T2 DSs for the period 1979–2021 are shown in Figures 2b and 2c. For T1, the frequency was the highest in April (63 events), followed by March (31) and May (24). For T2, the frequency was highest in April (202), followed by May (168) and March (144). During 1979–2021, there were no significant frequency trends for T1 DSs, but the T2 DSs showed a significant ($p < 0.01$) annual decrease of 4.2 events per decade (Figure 2f). Regarding DSs in 2021 (Figures 2a and 2d), the extremely high PM_{10} levels of northern China were associated with T1 DSs. The four spikes (March 15, March 28, April 16, and May 7) in PM_{10} concentrations were observed after the outbreak of T1 DS. Considering the strong temporal linkage and wide-ranging impact on air quality over northern China, the T1 type is inferred to have the greatest influence on air quality over the region.

Based on the clustering category shown in Figure 2a, we undertook composite analyses of the typical synoptic systems responsible for T1 and T2 DSs. Composites of geopotential height anomalies at 500 and 850 hPa, sea-level pressure anomalies, and associated wind anomalies are shown in Figure 3. From the mid-troposphere to the surface, strong cyclonic anomalies were observed over Mongolia and Inner Mongolia during the T1 DS, indicating the strong impact of the Mongolian cyclone (a mid-latitude cyclonic system over the region of 40°–50°N, 100°–115°E). With the eastern–southeastern migration of the cyclone, strong northwesterly winds following it were favorable for the outbreak of the DS when passing over the GD. During the T2 DS, significant wind shear

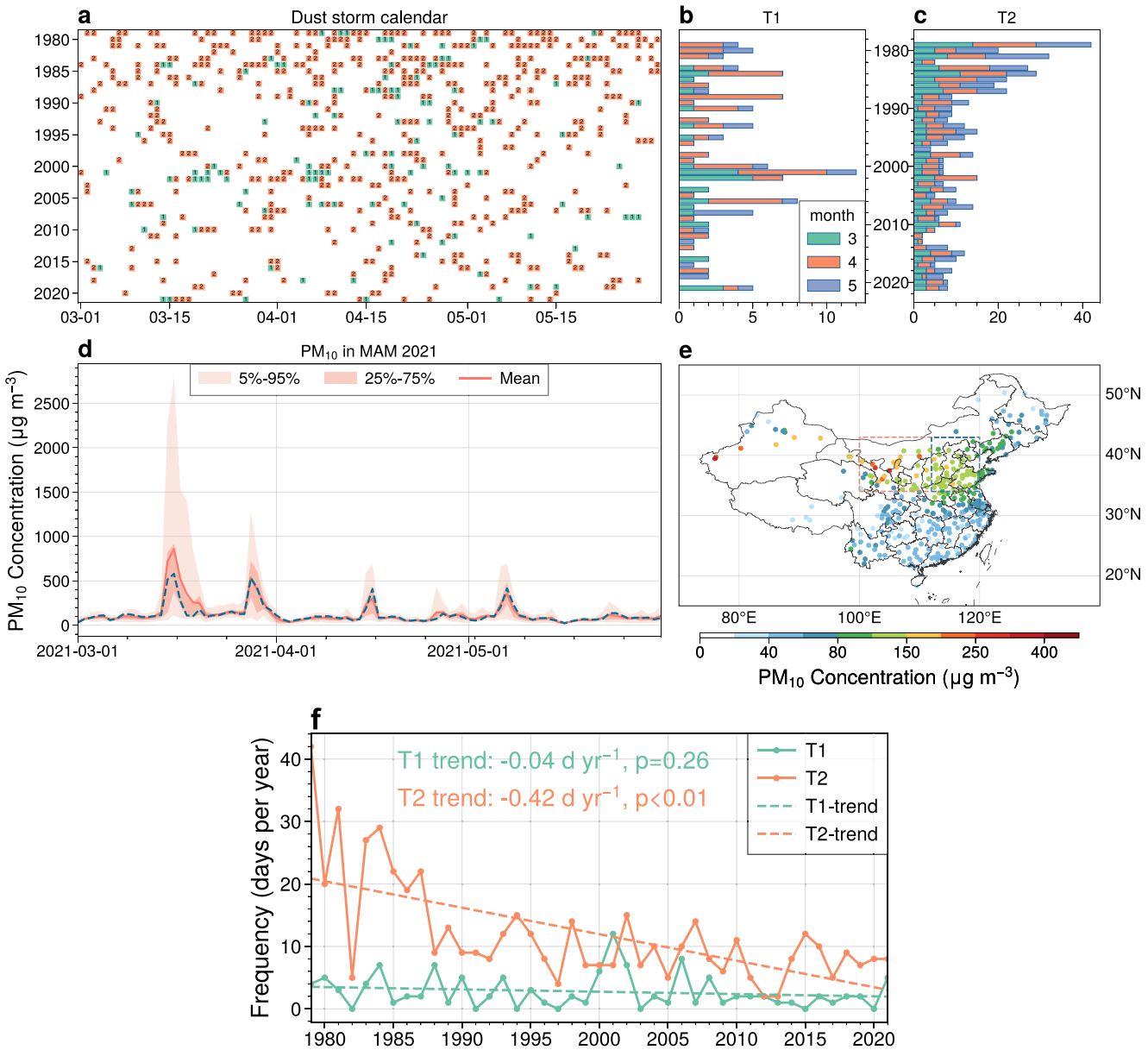

Figure 2. (a) Classified spring dust storm (DS) events during 1979–2021. (b), (c) Interannual variations in DS frequency for each month in spring for T1 and T2 DSs. (d) Evolution of PM_{10} concentrations averaged over the North China Plain [i.e., the area outlined by the blue rectangle in (e)] and northern China [red rectangle in (e)] during spring in 2021. (e) Spring mean PM_{10} concentrations in 2021. (f) Long-term variations in the frequency of T1 and T2 DSs during spring for the period 1979–2021. Dashed lines indicate linear regression trends; *p*-values denote statistical significance (Student's *t*-test).

at around 40°N latitude indicates the occurrence of a cold front (Figures 3d and 3f). The atmospheric pressure difference between southern warm air and northern cold air induced strong wind anomalies at the surface, raising dust from the TD into the atmosphere (Figure 3f).

3.2. Future Projections

Guided by the composited anomalies during T1 DSs, the daily meteorological field (averaged over the area indicated by blue and red rectangles in Figures 4a–4c) was used to generate time series for Z850, U10, and V10 (the Z850 and V10 time series were multiplied by −1 for convenience). The MCI was then constructed accordingly and was evaluated in several ways. In March (Figure 4) and April (Figure S7 in Supporting Information S1), MCI values of 80% and 62% for T1 DSs exceeded 1.8σ (Figures 4d) and 1.5σ (Figure S7d in Supporting

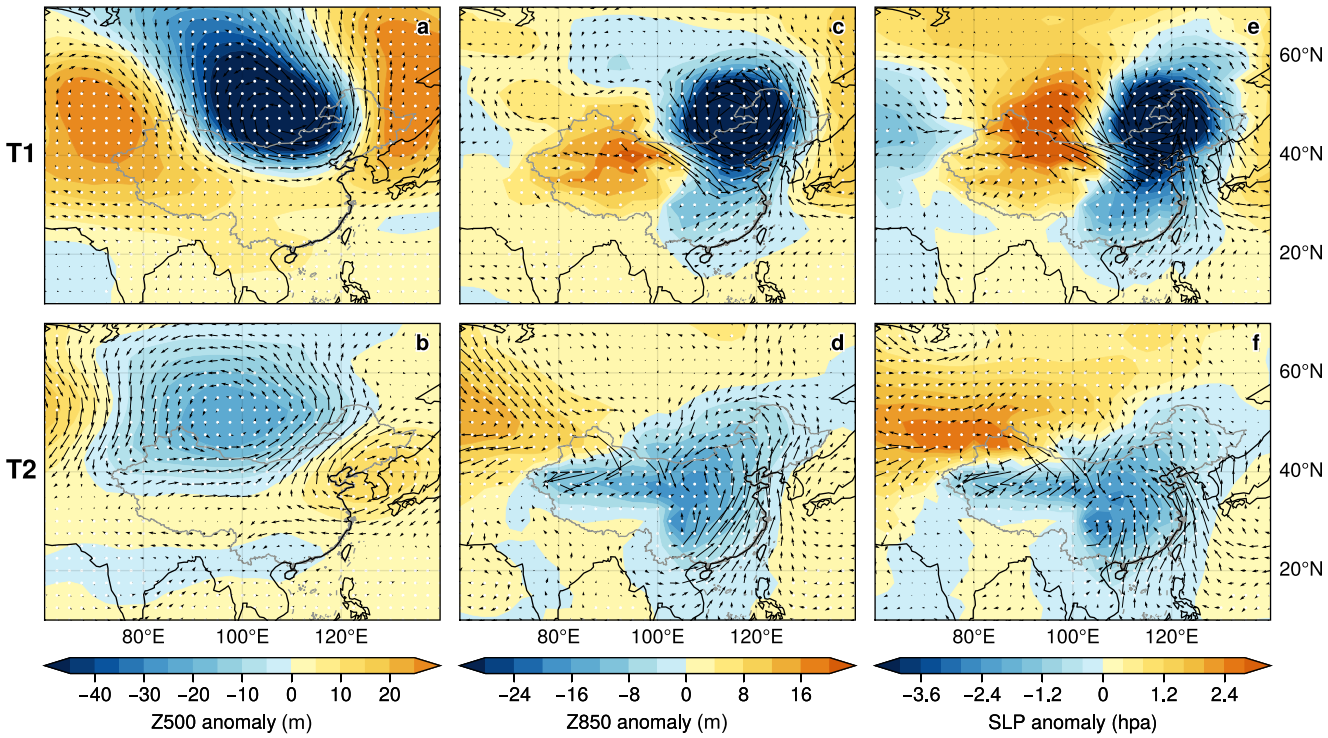

Figure 3. Weather conditions for the two dust storm (DS) types, T1 and T2. Composited anomalous weather patterns of (a), (b) geopotential height (m, shading) and winds (m s^{-1}, vectors) at 500 hPa; (c), (d) geopotential height (m), and winds (m s^{-1}) at 850 hPa; and (e), (f) sea-level pressure (hPa, shading) and winds (m s^{-1}) at 10 m. All anomalies are relative to the daily climatology over 1981–2010. White dots indicate that the circulation changes are significant at the 99% confidence level (Student's *t*-test).

Information S1), respectively (σ = standard deviation of the daily MCI during 1979–2021). For the whole period 1979–2021, the annual frequency of MCI values exceeding 1.8σ and 1.5σ may represent interannual variations in T1 DSs, with correlation coefficients of 0.70 and 0.65 for March and April, respectively (significant at the 99% level). We undertook the same analysis in May but found MCI alone could not well explain variations in T1 DSs (Figure S8 in Supporting Information S1). Mean NDVI values in May during 1979–2021 (Figure S9 in Supporting Information S1) increased significantly relative to March and April. A greater surface roughness due to higher vegetation coverage has been suggested to reduce friction velocity and thus restrain the outbreak of DSs (Mao et al., 2013). Earlier vegetation phenology under global warming (Fan et al., 2014) adds more uncertainty to future projections of May DSs. Considering the lowest occurrence (20%) of DSs in May, the impact of vegetation cover, and the complexity of phenology shifts under global warming, future changes in T1 DSs occurrence for only March and April were considered here.

Under the SSP585 scenario, 67% (12 of 18) of models projected increasing trends in the frequency of T1 DSs (MCI >1.8σ) in March (Figure S10a in Supporting Information S1). Aggregated over the 18 models, a weak ($P = 0.09$) increasing trend during 2020–2100 was obtained, with 0.03 days increase in T1 DSs per decade (Figure 5a). For April, the frequency of strong Mongolian cyclones decreased markedly, with the decreasing trend in T1 DS occurrence in April being −0.1 days per decade for 2020–2100 under the SSP585 scenario (Figure 5b). This result is supported by a strong inter-model consensus, with 89% (16 of 18) of models indicating decreased frequencies of T1 DSs (Figure S10b in Supporting Information S1). Considering that the decreasing trend in April is greater than the increasing trend in March, with T1 DSs occurring most frequently in April, we conclude that the frequency of spring DSs affecting northern China will decline under global warming.

With the implementation of carbon-neutral policies and a pledge to achieve net-zero CO_2 emissions by 2060, China is likely to follow the SSP126 scenario, under which T1 DS frequencies in both March and April exhibited no significant trends but rather fluctuated with decadal variability. The T1 DS frequency in March is projected to decrease from 2020 to 2040, after which it will increase to peak at around 2060 (Figure 5c). For April, there

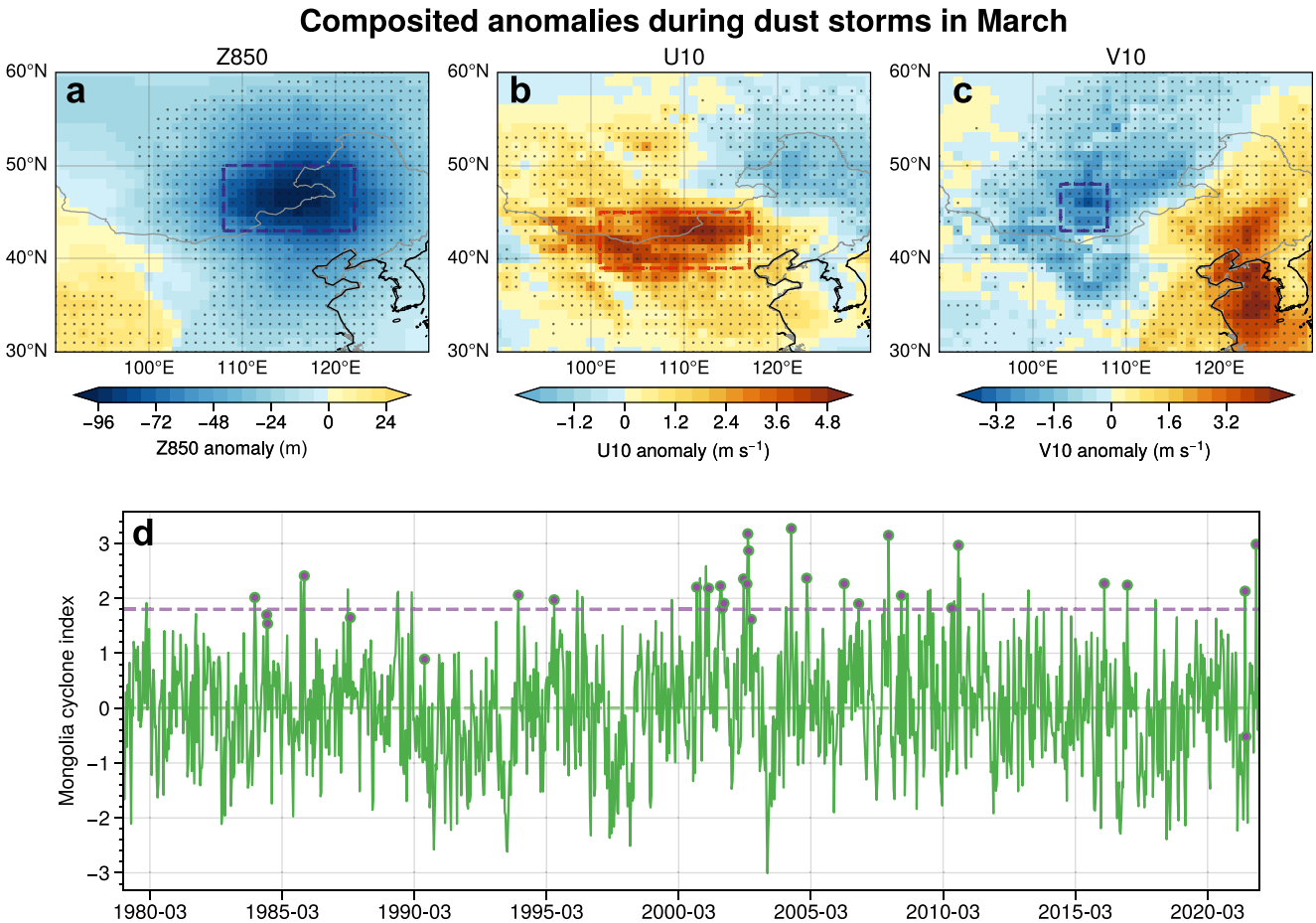

Figure 4. Composited anomalies of (a) geopotential height at 850 hPa (Z850), (b) zonal winds at 10 m (U10), and (c) meridional winds at 10 m (V10) during T1 DSs in March for the period 1979–2021. (d) Daily Mongolian Cyclone Index (MCI) in March based on Z850, U10, and V10 for 1979–2021. The dashed rectangles in (a)–(c) are selected regions to calculate time series for Z850, U10, and V10. The purple markers in (d) indicate T1 DS records and the purple dashed line denote the 1.8σ threshold.

is a slight increase before 2025, with T1 DSs entering a low-frequency period during 2025–2055, followed by a relatively high-occurrence period during 2055–2085 (Figure 5d).

3.3. Discussion

The two DS types exhibit significant differences in both long term trend and spatial pattern of the occurrences of DS. Although there is a consensus on the decreasing trend of DSs in northern China over the past decades (Guo et al., 2018; Qian et al., 2002; Zhu et al., 2008), our findings suggest that T1 DSs induced by Mongolian cyclone has no trend, and hence T2 DSs are primarily responsible for the declining trend of DSs in northern China. Such conclusion is supported by Zhu et al. (2008), who applied the Empirical Orthogonal Function analysis to the spring DS frequency during 1954–2007 and found no significant trend for the second leading mode (similar to our T1 DS characterized by high DS frequency in the Inner Mongolia). Compared to T2 DS from the TD, T1 DS has lower frequency of occurrence but plays a dominant role in the deterioration of air quality over northern China. T2 DSs are mainly from the TD, located in the Tarim Basin with its three sides surrounded by the mountains. Owing to its unique geography, the relatively weak easterlies at the surface could not easily transport TD dust particles outside the Tarim Basin (Chen et al., 2017). On the contrary, the terrain of the GD is mainly flat and high in elevation, and it is influenced by jet streams, which result in strong wind speeds in the upper atmosphere. The downward momentum transportation produced by the strong westerly jet with deep convective mixing can result in strong surface winds and low-level cyclogenesis and frontogenesis; Under these favorable conditions, the T1 DSs are likely to occur and are easily transported to downwind areas (Chen et al., 2017; Fan et al., 2018).

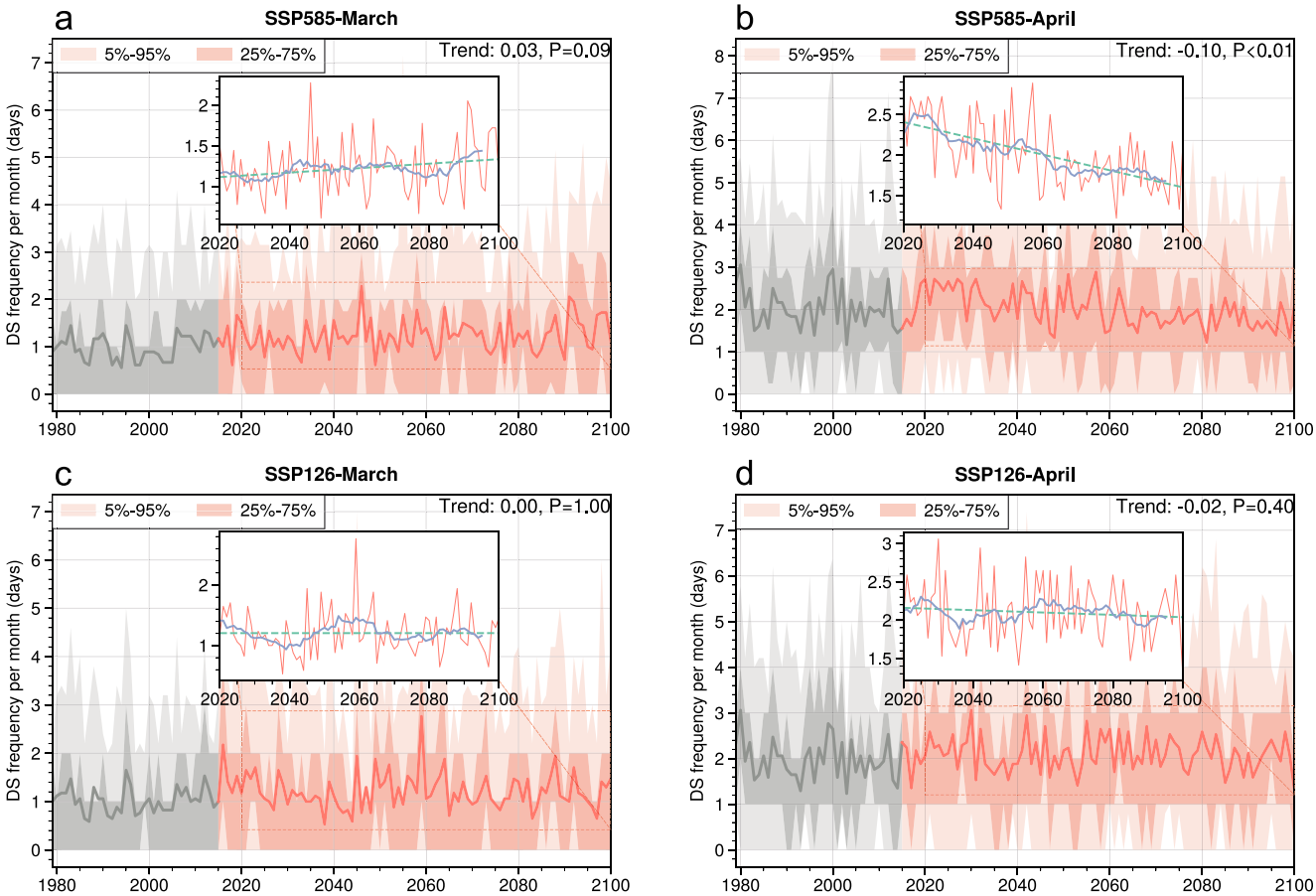

Figure 5. Future changes of dust storm (DS) frequency in March (a), (c) and April (b), (d) based on climate models under the SSP585 (a), (b) and SSP126 (c), (d) scenarios. Gray lines and shading indicate historical simulation frequencies for 1979–2015; red lines and shading indicate future variations for 2016–2100; green dashed lines indicate linear trends based on linear regression for 2020–2099; pale blue lines in insets indicate the 11-year moving average.

Therefore, the Mongolian cyclone driven T1 DSs from the GD have significant impacts on surface air quality over northern China.

Future trends of T1 DS occurrences differ between two future scenarios, with SSP585 showing a declining trend and SSP126 showing decadal variability. It is likely that climate-change effects on future DSs will be regulated by the amplitude of global warming. The SSP126 scenario is more likely to happen than the SSP585 scenario because of the proposed carbon-neutral policy (Liu et al., 2021), despite the fact that the SSP126 scenario's net-zero carbon emission is predicted to occur later than 2060. Therefore, future predictions of spring DSs should consider decadal variability as China takes the carbon-neutral path. It is also worthwhile to explore why the frequency of T1 DSs is decreasing under the SSP585 scenario. Several studies have revealed that the westerly jet stream (Chen et al., 2017; Zhu et al., 2008) and warming in the Mongolian Plateau (Qian et al., 2002) had significant impacts on the frequency of Mongolian cyclones. Zhu et al. (2008) demonstrated that the increases in surface air temperature in the region of 70–130°E, 45–65°N could reduce the number of Mongolian cyclones by inducing a weak westerly jet stream and weak atmospheric baroclinicity in northern China. We therefore investigated the future warming trends of surface air temperature under the SSP585 scenario and found large positive trends over the Mongolian Plateau for the years of 2020–2099 (Figure S11 in Supporting Information S1), which may explain in part the decreasing trend of T1 DSs frequency under the SSP585 scenario. For comparison, more than half of the models show no significant warming trends under the SSP126 scenario, while four models even predict cooling trends. These model discrepancies are inferred to contribute to the insignificant trend of DS frequency under the SSP126 scenario (Figure S12 in Supporting Information S1).

Apart from synoptic systems, the conditions of dust sources, particularly vegetation coverage, are also important factors in the occurrence of DSs. For example, DS frequency is the lowest in May due to more vegetation coverage over the dust storm region as compared to March and April (Figure S9 in Supporting Information S1). It was also reported that the frequency of spring dust storms in China had a higher correlation with NDVI in the previous summer than that in the spring of current year (Zou & Zhai, 2004). We therefore investigated the potential correlation between NDVI and T1 or T2 DSs during MAM and the preceding seasons of December–February, September–November, and June–August (Figure S13 in Supporting Information S1). A weak correlation is found between NDVI and T1 DSs, suggesting that the T1 DSs driven by Mongolian cyclone are more susceptible to synoptic systems than to dust source conditions. As for T2, no correlations are identified over the TD, whereas significantly negative correlations exist over the western GD (or the Hexi Corridor). Because the TD is a nonvegetated desert with fine dust particles, the occurrences of spring DSs are unrelated to the vegetation. The negative correlations in western GD indicate NDVI play a non-negligible role in DS occurrence despite the influence of cold front. In addition to the mean vegetation coverage during dust season, earlier vegetation growth in spring may have a dampening impact on DS frequency in Inner Mongolia (Li et al., 2015), and such effects are likely to play important roles, given the observation of earlier spring phenology associated with winter and spring warming (Piao et al., 2019). Therefore, the earlier onset of vegetation green-up in a warming climate may suppress the development of DSs. It should also be noted that global warming may bring in more intensive synoptic systems. Extreme DSs are likely to occur under these weather conditions, especially if they coincide with favorable dust source conditions. For example, the lowest vegetation coverage and the second strongest Mongolian cyclone among recent decade in spring 2021 contributed to the super DSs on 15 March 2021 in northern China (Yin et al., 2021). Such dual effect of climate change on DS occurrence should be further studied.

4. Conclusion

Based on K-means clustering, two DS types were identified from 632 spring dust events in northwestern and northern China, accounting for 18.7% and 81.3% of events, respectively. T1 DSs, generated mainly in the GD, is identified as the predominant DS type influencing air quality in northern China. T2 DSs influence mainly northwestern China. During 1979–2021, T1 DSs displayed no significant trends in the frequency of occurrence, while T2 DSs exhibited a decreasing trend at a rate of 4.2 events per decade. The major synoptic systems driving T1 and T2 DSs are Mongolian cyclones and cold fronts, respectively. MCI were established to track interannual variations in T1 DS frequency, with T1 DSs projected to decrease during 2020–2100 under the SSP585 scenario. No significant trends were detected for the frequency of T1 DSs under the SSP126 scenario, but decadal variability associated with the mitigation of global warming may have import implications for future DS prediction.

Data Availability Statement

Surface meteorological observations were obtained from https://www.ncei.noaa.gov/data/global-hourly/access/. PM_{10} observations were obtained from http://106.37.208.233:20035/. The ERA5 reanalysis data are available at https://cds.climate.copernicus.eu/cdsapp#!/dataset/reanalysis-era5-pressure-levels?tab=form and https://cds.climate.copernicus.eu/cdsapp#!/dataset/reanalysis-era5-single-levels?tab=form. Aerosol optical depth from Moderate Resolution Imaging Spectroradiometer aerosol products were obtained from https://ladsweb.modaps.eosdis.nasa.gov/search/. CMIP6 outputs are available from https://esgf-node.llnl.gov/search/cmip6/.

Acknowledgments
This work was supported by the National Natural Science Foundation of China (Grant Nos. 42021004, 91744311, and 42088101), the Major Research Plan of the National Social Science Foundation (Grant No. 18ZDA052), the Guangdong Major Project of Basic and Applied Basic Research (Grant No. 2020B0301030004) and the Natural Science Foundation of Jiangsu Higher Education Institutions of China (Grant 20KJB170002).

References

Agel, L., Barlow, M., Skinner, C., Colby, F., & Cohen, J. (2021). Four distinct Northeast US heat wave circulation patterns and associated mechanisms, trends, and electric usage. *NPJ Climate and Atmospheric Science*, *4*(1), 31. https://doi.org/10.1038/s41612-021-00186-7

Cai, W., Li, K., Liao, H., Wang, H., & Wu, L. (2017). Weather conditions conducive to Beijing severe haze more frequent under climate change. *Nature Climate Change*, *7*(4), 257–262. https://doi.org/10.1038/nclimate3249

Chang, W., & Zhan, J. (2017). The association of weather patterns with haze episodes: Recognition by PM2.5 oriented circulation classification applied in Xiamen, Southeastern China. *Atmospheric Research*, *197*, 425–436. https://doi.org/10.1016/j.atmosres.2017.07.024

Chen, S., Huang, J., Li, J., Jia, R., Jiang, N., Kang, L., et al. (2017). Comparison of dust emissions, transport, and deposition between the Taklimakan Desert and Gobi Desert from 2007 to 2011. *Science China Earth Sciences*, *60*(7), 1338–1355. https://doi.org/10.1007/s11430-016-9051-0

Ding, R., Li, J., Wang, S., & Ren, F. (2005). Decadal change of the spring dust storm in northwest China and the associated atmospheric circulation. *Geophysical Research Letters*, *32*(2). https://doi.org/10.1029/2004gl021561

Engelstaedter, S., Kohfeld, K. E., Tegen, I., & Harrison, S. P. (2003). Controls of dust emissions by vegetation and topographic depressions: An evaluation using dust storm frequency data. *Geophysical Research Letters*, *30*(6). https://doi.org/10.1029/2002gl016471

Fan, B., Guo, L., Li, N., Chen, J., Lin, H., Zhang, X., et al. (2014). Earlier vegetation green-up has reduced spring dust storms. *Scientific Reports*, *4*(1), 6749. https://doi.org/10.1038/srep06749

Fan, K., Xie, Z., Wang, H., Xu, Z., & Liu, J. (2018). Frequency of spring dust weather in North China linked to sea ice variability in the Barents Sea. *Climate Dynamics*, *51*(11), 4439–4450. https://doi.org/10.1007/s00382-016-3515-7

Fussell, J. C., & Kelly, F. J. (2021). Mechanisms underlying the health effects of desert sand dust. *Environment International*, *157*, 106790. https://doi.org/10.1016/j.envint.2021.106790

Griffin, D. W., Kellogg, C. A., & Shinn, E. A. (2001). Dust in the wind: Long range transport of dust in the atmosphere and its implications for global public and ecosystem health. *Global Change & Human Health*, *2*(1), 20–33. https://doi.org/10.1023/A:1011910224374

Guan, Q., Sun, X., Yang, J., Pan, B., Zhao, S., & Wang, L. (2017). Dust storms in northern China: Long-term spatiotemporal characteristics and climate controls. *Journal of Climate*, *30*(17), 6683–6700. https://doi.org/10.1175/jcli-d-16-0795.1

Guo, L., Fan, B., Zhang, F., Jin, Z., & Lin, H. (2018). The clustering of severe dust storm occurrence in China from 1958 to 2007. *Journal of Geophysical Research: Atmospheres*, *123*(15), 8035–8046. https://doi.org/10.1029/2018jd029042

He, L., Hao, X., Li, H., & Han, T. (2021). How do extreme summer precipitation events over eastern China subregions change? *Geophysical Research Letters*, *48*(5), e2020GL091849. https://doi.org/10.1029/2020gl091849

Hersbach, H., Bell, B., Berrisford, P., Hirahara, S., Horányi, A., Muñoz-Sabater, J., et al. (2020). The ERA5 global reanalysis. *Quarterly Journal of the Royal Meteorological Society*, *146*(730), 1999–2049. https://doi.org/10.1002/qj.3803

Huang, J., Yu, H., Guan, X., Wang, G., & Guo, R. (2016). Accelerated dryland expansion under climate change. *Nature Climate Change*, *6*(2), 166–171. https://doi.org/10.1038/nclimate2837

Huang, X.-X., Wang, T.-J., Jiang, F., Liao, J.-B., Cai, Y.-F., Yin, C.-Q., et al. (2013). Studies on a severe dust storm in East Asia and its impact on the air quality of Nanjing, China. *Aerosol and Air Quality Research*, *13*(1), 179–193. https://doi.org/10.4209/aaqr.2012.05.0108

Ichinose, T., Yoshida, S., Hiyoshi, K., Sadakane, K., Takano, H., Nishikawa, M., et al. (2008). The effects of microbial materials adhered to Asian sand dust on allergic lung inflammation. *Archives of Environmental Contamination and Toxicology*, *55*(3), 348–357. https://doi.org/10.1007/s00244-007-9128-8

Ji, L., & Fan, K. (2019). Climate prediction of dust weather frequency over northern China based on sea-ice cover and vegetation variability. *Climate Dynamics*, *53*(1), 687–705. https://doi.org/10.1007/s00382-018-04608-w

Lee, E.-H., & Sohn, B.-J. (2009). Examining the impact of wind and surface vegetation on the Asian dust occurrence over three classified source regions. *Journal of Geophysical Research*, *114*(D6). https://doi.org/10.1029/2008jd010687

Li, H., Yang, Y., Wang, H., Li, B., Wang, P., Li, J., & Liao, H. (2021). Constructing a spatiotemporally coherent long-term PM2.5 concentration dataset over China during 1980–2019 using a machine learning approach. *Science of the Total Environment*, *765*, 144263. https://doi.org/10.1016/j.scitotenv.2020.144263

Li, J., Hao, X., Liao, H., Hu, J., & Chen, H. (2021). Meteorological impact on winter PM2.5 pollution in Delhi: Present and future projection under a warming climate. *Geophysical Research Letters*, *48*(13), e2021GL093722. https://doi.org/10.1029/2021gl093722

Li, J., Liao, H., Hu, J., & Li, N. (2019). Severe particulate pollution days in China during 2013–2018 and the associated typical weather patterns in Beijing-Tianjin-Hebei and the Yangtze River Delta regions. *Environmental Pollution*, *248*, 74–81. https://doi.org/10.1016/j.envpol.2019.01.124

Li, N., Guo, L., & Fan, B. (2015). A new perspective on understanding the reduced spring dust storm frequency in Inner Mongolia, China. *International Journal of Disaster Risk Science*, *6*(3), 216–225. https://doi.org/10.1007/s13753-015-0062-5

Liao, H., & Seinfeld, J. H. (1998). Radiative forcing by mineral dust aerosols: Sensitivity to key variables. *Journal of Geophysical Research*, *103*(D24), 31637–31645. https://doi.org/10.1029/1998jd200036

Liu, S., Xing, J., Sahu, S. K., Liu, X., Liu, S., Jiang, Y., et al. (2021). Wind-blown dust and its impacts on particulate matter pollution in northern China: Current and future scenario. *Environmental Research Letters*. Retrieved from http://iopscience.iop.org/article/10.1088/1748-9326/ac31ec

Liu, X., Yin, Z.-Y., Zhang, X., & Yang, X. (2004). Analyses of the spring dust storm frequency of northern China in relation to antecedent and concurrent wind, precipitation, vegetation, and soil moisture conditions. *Journal of Geophysical Research*, *109*(D16). https://doi.org/10.1029/2004jd004615

Mao, R., Ho, C.-H., Feng, S., Gong, D.-Y., & Shao, Y. (2013). The influence of vegetation variation on Northeast Asian dust activity. *Asia-Pacific Journal of Atmospheric Sciences*, *49*(1), 87–94. https://doi.org/10.1007/s13143-013-0010-5

Meng, L., Yang, X., Zhao, T., He, Q., Lu, H., Mamtimin, A., et al. (2019). Modeling study on three-dimensional distribution of dust aerosols during a dust storm over the Tarim Basin, Northwest China. *Atmospheric Research*, *218*, 285–295. https://doi.org/10.1016/j.atmosres.2018.12.006

Pei, L., Yan, Z., Sun, Z., Miao, S., & Yao, Y. (2018). Increasing persistent haze in Beijing: Potential impacts of weakening East Asian winter monsoons associated with northwestern Pacific sea surface temperature trends. *Atmospheric Chemistry and Physics*, *18*(5), 3173–3183. https://doi.org/10.5194/acp-18-3173-2018

Piao, S., Liu, Q., Chen, A., Janssens, I. A., Fu, Y., Dai, J., et al. (2019). Plant phenology and global climate change: Current progresses and challenges. *Global Change Biology*, *25*(6), 1922–1940. https://doi.org/10.1111/gcb.14619

Pu, B., & Ginoux, P. (2018). How reliable are CMIP5 models in simulating dust optical depth? *Atmospheric Chemistry and Physics*, *18*(16), 12491–12510. https://doi.org/10.5194/acp-18-12491-2018

Qian, W., Quan, L., & Shi, S. (2002). Variations of the dust storm in China and its climatic control. *Journal of Climate*, *15*(10), 1216–1229. https://doi.org/10.1175/1520-0442(2002)015<1216:votdsi>2.0.co;2

Riahi, K., van Vuuren, D. P., Kriegler, E., Edmonds, J., O'Neill, B. C., Fujimori, S., et al. (2017). The shared socioeconomic pathways and their energy, land use, and greenhouse gas emissions implications: An overview. *Global Environmental Change*, *42*, 153–168. https://doi.org/10.1016/j.gloenvcha.2016.05.009

Shi, L., Zhang, J., Yao, F., Zhang, D., & Guo, H. (2020). Temporal variation of dust emissions in dust sources over Central Asia in recent decades and the climate linkages. *Atmospheric Environment*, *222*, 117176. https://doi.org/10.1016/j.atmosenv.2019.117176

Sokolik, I. N., & Toon, O. B. (1996). Direct radiative forcing by anthropogenic airborne mineral aerosols. *Nature*, *381*(6584), 681–683. https://doi.org/10.1038/381681a0

Sun, J., Zhang, M., & Liu, T. (2001). Spatial and temporal characteristics of dust storms in China and its surrounding regions, 1960–1999: Relations to source area and climate. *Journal of Geophysical Research*, *106*(D10), 10325–10333. https://doi.org/10.1029/2000jd900665

Wu, C., Lin, Z., Liu, X., Li, Y., Lu, Z., & Wu, M. (2018). Can climate models Reproduce the decadal change of dust aerosol in East Asia? *Geophysical Research Letters*, *45*(18), 9953–9962. https://doi.org/10.1029/2018gl079376

Xu, C., Guan, Q., Lin, J., Luo, H., Yang, L., Tan, Z., et al. (2020). Spatiotemporal variations and driving factors of dust storm events in northern China based on high-temporal-resolution analysis of meteorological data (1960–2007). *Environmental Pollution*, *260*, 114084. https://doi.org/10.1016/j.envpol.2020.114084

Yao, W., Gui, K., Wang, Y., Che, H., & Zhang, X. (2021). Identifying the dominant local factors of 2000–2019 changes in dust loading over East Asia. *Science of The Total Environment*, *777*, 146064. https://doi.org/10.1016/j.scitotenv.2021.146064

Yin, Z., Wan, Y., Zhang, Y., & Wang, H. (2021). Why super sandstorm 2021 in North China. *National Science Review*. https://doi.org/10.1093/nsr/nwab165

Zhang, D., Huang, Y., Zhou, B., & Wang, H. (2021). Is there Interdecadal variation in the South Asian high? *Journal of Climate*, *34*(20), 8089–8103. https://doi.org/10.1175/jcli-d-21-0059.1

Zhao, A., Ryder, C. L., & Wilcox, L. J. (2022). How well do the CMIP6 models simulate dust aerosols? *Atmospheric Chemistry and Physics*, *22*(3), 2095–2119. https://doi.org/10.5194/acp-22-2095-2022

Zhao, C., Dabu, X., & Li, Y. (2004). Relationship between climatic factors and dust storm frequency in Inner Mongolia of China. *Geophysical Research Letters*, *31*(1). https://doi.org/10.1029/2003gl018351

Zhu, C., Wang, B., & Qian, W. (2008). Why do dust storms decrease in northern China concurrently with the recent global warming? *Geophysical Research Letters*, *35*(18). https://doi.org/10.1029/2008gl034886

Zong, Q., Mao, R., Gong, D.-Y., Wu, C., Pu, B., Feng, X., & Sun, Y. (2021). Changes in dust activity in spring over East Asia under a global warming scenario. *Asia-Pacific Journal of Atmospheric Sciences*, *57*(4), 839–850. https://doi.org/10.1007/s13143-021-00224-7

Zou, X. K., & Zhai, P. M. (2004). Relationship between vegetation coverage and spring dust storms over northern China. *Journal of Geophysical Research*, *109*(D3). https://doi.org/10.1029/2003jd003913